RESEARCH ARTICLE
doi: 10.2306/scienceasia1513-1874.2022.047

ScienceAsia 48 (2022): **270–277**

Analysis of novel prognostic markers of oral squamous cell carcinoma at the transcriptome-wide level

Li Kunshan[a], **Liu Yuanhang**[b], **Sun Jieming**[c], **Qiu Junping**[c], **Wang Wenjing**[a], **Qiu Yongle**[a,*]

[a] Department of Stomatology, Fourth Affiliated Hospital, Hebei Medical University, Shijiazhuang, Hebei 050000 China
[b] Department of Stomatology, Second Hospital of Shijiazhuang, Shijiazhuang, Hebei 050000 China
[c] Department of Stomatology, Xianghe County People's Hospital, Langfang, Hebei 065400 China

*Corresponding author, e-mail: dentist2020@163.com

Received 2 Aug 2021, Accepted 26 Nov 2021
Available online 28 Feb 2022

ABSTRACT: Patients with oral squamous cell carcinoma (OSCC) have a poor prognosis. The molecular mechanism of OSCC progression remains unclear. The aim of this study was to explore specific prognostic biomarkers of OSCC at the transcriptome-wide level. A total of 158 differentially expressed long non-coding RNAs (lncRNAs), including 85 *cis*-acting and 10 *trans*-acting differentially expressed lncRNAs, were screened in OSCC tissues compared with adjacent normal tissues. Both *cis*- and *trans*-target genes of differentially expressed lncRNAs were enriched in pathways associated with cancer progression. Additionally, 25 differentially expressed mRNAs were screened. Overlapping analysis of differential protein-coding genes with the *cis*- and *trans*-target genes of differentially expressed lncRNAs indicated that KIF19 was the only *trans*-acting gene of differentially expressed lncRNA 'ENST00000626052' (named ENSTa). ENSTa was down-regulated in OSCC tissues and cells, and its low expression corresponded to a poor prognosis in OSCC. KIF19 was highly expressed in OSCC tissues and cells. Patients with high expression of KIF19 had a poor prognosis. Cellular experiments showed that KIF19 expression and cell proliferation were inhibited in cells overexpressing ENSTa. However, KIF19 overexpression counteracted the effect of ENSTa overexpression on cell proliferation. In conclusion, ENSTa regulated the *trans*-acting KIF19 gene in the inhibition of the progression of OSCC, thus they could be suggested as novel biomarkers for OSCC.

KEYWORDS: oral squamous cell carcinoma, prognostic biomarker, long-noncoding RNA, *trans*-acting gene, differential expression

INTRODUCTION

Oral squamous cell carcinoma (OSCC) is one of the most common malignant tumors of the oral and maxillofacial region [1, 2]. The prevalence of OSCC is higher in males than females [3]. OSCC develops from oral epithelial cells and is associated with high morbidity and mortality [4]. Common clinical treatments for OSCC include surgery, chemotherapy and radiotherapy [1, 2]. Neoadjuvant chemotherapy is systemic chemotherapy administered prior to local treatment such as surgery or radiotherapy. Neoadjuvant chemotherapy can reduce tumor stage, reduce tumor volume and destroy some metastatic cells [5]. The efficacy of neoadjuvant chemotherapy in the treatment of OSCC remains controversial [6]. The outcome of OSCC treatment remains unsatisfactory with a 5-year survival rate less than 50% [7, 8]. How to improve the diagnosis and treatment options for OSCC is an important challenge. Therefore, it is important to explore the molecular mechanisms underlying the development of OSCC.

About 75% of genes in the human genome are transcribed as non-coding RNAs [9, 10]. Long non-coding RNAs (lncRNAs) are greater than 200 bp in length, which can regulate target gene expression in *cis*- or *trans*-acting [10–14]. *Cis*-acting refers to regulation of gene expression in the vicinity of lncRNA. For *trans*-acting, lncRNAs regulate the expression of remote target genes to perform a range of functions in cells [15]. *Cis*- and *trans*-acting of aberrantly expressed lncRNAs plays an important role in cancer development [16–18]. For example, lncRNA RP11.513I15.6 promotes non-small cell lung cancer progression by inhibiting HMGA1 expression through *cis*-acting [17]. RUNX1-IT1 acts as a pro-oncogene in pancreatic cancer and promotes C-FOS expression by recruiting RUNX1 to the C-FOS gene promoter via *trans*-acting [18]. Exploring the aberrant lncRNAs with *cis*- and *trans*-acting in OSCC is beneficial for advancing the study of OSCC developmental mechanisms.

The objective of this research was to investigate the prognostic signature of OSCC at the transcriptome-wide level. Differentially expressed lncRNAs and corresponding target genes with *cis*- or *trans*-acting in OSCC were identified, and the effects of these lncRNAs and target genes on prognosis and cell proliferation were analyzed. This study will contribute to the discovery of new biomarkers for diagnosis and treatment of OSCC.

MATERIALS AND METHODS

Clinical samples

Forty-five patients with OSCC treated from April 2019 to June 2020 in Fourth Affiliated Hospital of Hebei

Medical University were enrolled in this study. The clinical characteristics of the 45 patients were shown in Table S1. All patients were pathologically diagnosed with OSCC. None of the enrolled patients had received radiation and had no history of surgery. All of the 45 patients were treated with neoadjuvant chemotherapy followed by surgery. After the patients signed the written informed consent, OSCC tissue samples and corresponding normal control tissue samples were collected. The tissue samples were stored in liquid nitrogen prior to RNA extraction. Four pairs of OSCC and normal control tissues from patients undergoing neoadjuvant chemotherapy were selected for microarray analysis. All of the 45 pairs of samples were used for qRT-PCR assay. This study was approved by the Fourth Affiliated Hospital of Hebei Medical University Ethics Committee.

Microarray analysis

The RNeasy micro kit (Qiagen GmbH, Hilden, Germany) and the RNase-Free DNase set (Qiagen GmBH, Hilden, Germany) were used for the extraction and purification of total RNA from 4 pairs of OSCC and the corresponding control tissue samples. LncRNA and mRNA expression profiles were detected using Agilent-078298 human ceRNA array (4×180K) according to the manufacturer's instructions. The chip was scanned using an Agilent Microarray scanner (Agilent Technologies, Inc., California, USA). The raw data were normalized by the "Limma" package in the R software with Quantile algorithm. The normalized data were screened for differentially expressed genes and statistical significance. Log_2 fold Change $\geqslant 1$ and $\log_2$ fold Change $\leqslant -1$ indicated up-regulation and down-regulation of differentially expressed genes, respectively; p-values < 0.05 indicated a significant difference.

Prediction of *cis*- and *trans*-target genes of lncRNA

The gene with a distance less than 10 kb from lncRNA was selected as the *cis*-target gene. The sequences with complementarity or similarity in sequence were selected by blast. Then, the complementary energy between the 2 sequences was calculated using RNAplex. Sequence with e $\leqslant -30$ was selected as the *trans*-target gene. Chromosomal distribution of lncRNA and target genes and interactions were performed by using TBtools software [19].

Kyoto encyclopedia of genes and genomes (KEGG) enrichment

KEGG enrichment was carried out by the Fisher exact test in the PANTHER classification system and clusterProfiler package of R. The criteria for selection were that the number of differentially expressed genes in a term was not less than 2 and p-values < 0.05.

Cell culture and transfection

Normal human oral keratinocyte cell line (NOK) was obtained from Cell Bank of the Chinese Academy of Sciences (Shanghai, China). OSCC cell lines (CAL-27, SCC-9 and SSC-25) were purchased from American Type Culture Collection (ATCC; VA, USA). All of cells were maintained in Dulbecco's modified medium (DMEM; Invitrogen, CA, USA) with 10% fetal bovine serum (FBS; Invitrogen).

ENSTa and KIF19 sequences were generated and then cloned into pcDNA3.1 plasmid (Invitrogen) to obtain the recombinant plasmids (pcDNA3.1-ENSTa and pcDNA3.1-KIF19). The recombinant plasmids or pcDNA3.1 plasmid was transfected into CAL-27 and SCC-9 cells according to the protocol of Lipofectamine 3000 (Invitrogen).

qRT-PCR

Total RNA was extracted from 45 tissue pairs or OSCC cells using TRIzol reagent (Thermo Fischer, MA, USA). PrimeScript RT reagent kit with gDNA Eraser (Thermo Fischer, USA) was used for reverse transcription. SYBR Green Fast qPCR Mix (Takara, Dalian, China) was used for qRT-PCR reaction. The conditions for the reverse transcription reaction were as follows: 25 °C for 10 min, 50 °C for 45 min and 85 °C for 5 min. The conditions for the qRT-PCR reaction were 95 °C for 3 min, 95 °C for 10 s, followed by 58 °C for 40 s (40 cycles) and 72 °C for 10 min. The primers used in this study were as follows: ENSTa: forward, 5′-CGCAGCTTGCACAGAAGGTA-3′; reverse, 5′-GAACTGCTGGCGGTTGAATC-3′. KIF19: forward, 5′-ACCCTCATCGCCCATAAAGTG-3′; reverse, 5′-TCGAACAGGTAGGACTTCTCC-3′. GAPDH: forward, 5′-GGAGCGAGATCCCTCCAAAAT-3′; reverse, 5′-GGCTGTTGTCATACTTCTCATGG-3′. GAPDH was selected as the internal control. $2^{-\Delta\Delta Cq}$ method was applied for the relative expression calculation. All experiments were replicated 3 times.

Cell proliferation assay

The cell counting kit-8 (CCK-8; Dojindo, Japan) was used for cell proliferation detection. After transfection, CAL-27 and SCC-9 cells were seeded into 96-well plates with 1×10^4 cells/well. CCK-8 regent (10 μl) was added into each well after culturing for 0, 1, 2 and 3 days. Then, cells were continuously cultured for 2 h at 37 °C. The absorbance at 450 nm was measured using a spectrophotometer (BioTek Instruments, CA, USA).

Statistical analysis

Statistical analysis was performed using GraphPad Prism 7.0. Differences among groups were compared by Student's t-test or one-way ANOVA. Kaplan-Meier method and log-rank t-test were applied for prognostic analysis using R based on The Cancer Genome Atlas

(TCGA) database. p-values < 0.05 were considered statistically significant.

RESULTS

Screening of differentially expressed lncRNAs and functional analysis of their target genes

The microarray detected a total of 158 differentially expressed lncRNAs (Fig. 1a). Heat map of the 158 differentially expressed lncRNAs was shown in Fig. 1b. To gain insight into the function of differentially expressed lncRNAs, the *cis*- and *trans*-target genes of differentially expressed lncRNAs were predicted. There were 85 *cis*- and 474 *trans*-target genes of the differentially expressed lncRNAs. KEGG analysis showed that the *cis*-target genes were mainly enriched in Ras signaling pathway, PPAR signaling pathway, focal adhesion and MAPK signaling pathway, etc (Fig. 1c). The *trans*-target genes were enriched in the pathway related to cancer cell apoptosis, autophagy and mTOR signaling pathway (Fig. 1d).

Distribution of differentially expressed lncRNAs with *cis*- and *trans*-acting on chromosomes

The distribution of 158 differentially expressed lncRNAs on chromosomes was analyzed. Differentially expressed lncRNAs were distributed on the X, Y and 1–22 chromosomes (Fig. 2a). There were 85 differentially expressed lncRNAs with *cis*-acting distributed on all chromosomes except the Y chromosome (Fig. 2b). A total of 10 lncRNAs with *trans*-acting were located on chromosomes 2, 6, 11, 12, 16, 17 and 19 (Fig. 2c). However, the *trans*-target genes were present on all chromosomes except for Y chromosome (Fig. 2c).

Overlapping analysis of *cis*- and *trans*-target genes of differentially expressed lncRNAs and protein-coding genes

A total of 25 353 mRNAs were detected by microarray, of which 25 mRNAs differed significantly in OSCC tissues compared with normal tissues (Fig. 3a,b). There was no intersection between *cis*-target genes of differentially expressed lncRNAs and protein-coding genes (Fig. 3c). Only one of the *trans*-regulatory genes, KIF19, was overlapped with the differential protein-coding gene (Fig. 3c). Hence, we focused on KIF19 and its *cis*-acting lncRNA (ENSTa).

Prognostic and expression analysis of ENSTa and KIF19

Based on data from TCGA, the effect of KIF19 and ENSTa expression on disease-free survival (DFS) of OSCC patients was analyzed using Kaplan-Meier curves. Patients from TCGA database were grouped into high- and low-expression group according to the quartiles. High expression of ENSTa had a positive impact on the prognosis of OSCC patients (Fig. 4a) whereas the high expression of KIF19 had a negative impact on the prognosis of OSCC patients (Fig. 4b). The expression of ENSTa and KIF19 in 45 pairs of tissues was detected. ENSTa was significantly down-regulated in OSCC tissues, while KIF19 was significantly up-regulated (Fig. 4c-d). Similarly, the expression of ENSTa in OSCC cells was notably lower than that in NOK cell (Fig. 4e). However, KIF19 expression in OSCC cells was obviously higher than NOK cell (Fig. 4f).

Effect of ENSTa and KIF19 on OSCC cells

The expression of ENSTa in ENSTa overexpressing cells was significantly higher than that in control cells (Fig. 5a). KIF19 expression was down-regulated in CAL-27 and SCC-9 cells transfected with pcDNA3.1-ENSTa, which verified the *trans*-acting between ENSTa and KIF19 (Fig. 5b). In addition, KIF19 expression was significantly elevated after overexpression of KIF19 in ENSTa overexpressing cells (Fig. 5b). As shown in Fig. 5c,d, ENSTa overexpression resulted in decreased cell proliferation. However, overexpression of KIF19 reversed the inhibitory effect of ENSTa overexpression on proliferation of CAL-27 and SCC-9 cells (Fig. 5c-d).

DISCUSSION

OSCC is highly malignant with high metastasis and recurrence rates [4, 20]. The 5-year survival of OSCC is less than 50% [7, 8]. Exploring the molecular mechanisms regulating the progression of OSCC has positive implications for improving clinical treatment strategies. In this study, transcriptional profiles of OSCC and adjacent normal tissues were analyzed, and 158 differentially expressed lncRNAs and 25 differentially expressed mRNAs were identified.

LncRNAs can regulate target gene expression at multiple levels such as epigenetic, transcriptional and post-transcriptional levels. According to the relative position of lncRNAs and target genes on chromosome, the interaction between lncRNAs and target genes can be divided into *cis*- and *trans*-acting. *Cis*- and *trans*-acting of lncRNAs play an important role in cancer progression [16–18]. In this study, we predicted *cis*- and *trans*-acting genes of 158 differentially expressed lncRNAs and found that there were 85 differentially expressed lncRNAs regulating 85 target genes in *cis*, and 10 differentially expressed lncRNAs regulated 474 target genes in *trans*. *Cis*-target genes were enriched in Ras signaling pathway, PPAR signaling pathway, focal adhesion and MAPK signaling pathway. *Trans*-target genes were enriched in apoptosis, autophagy and mTOR signaling pathway. The enrichment pathways of both *cis*- and *trans*-target genes were closely related to the progression of OSCC. Interestingly, the Y chromosome was devoid of both *cis*- and *trans*-acting differentially expressed lncRNAs as well as the corresponding target genes.

To further understand the role of abnormally expressed lncRNAs in OSCC, we conducted an overlap-

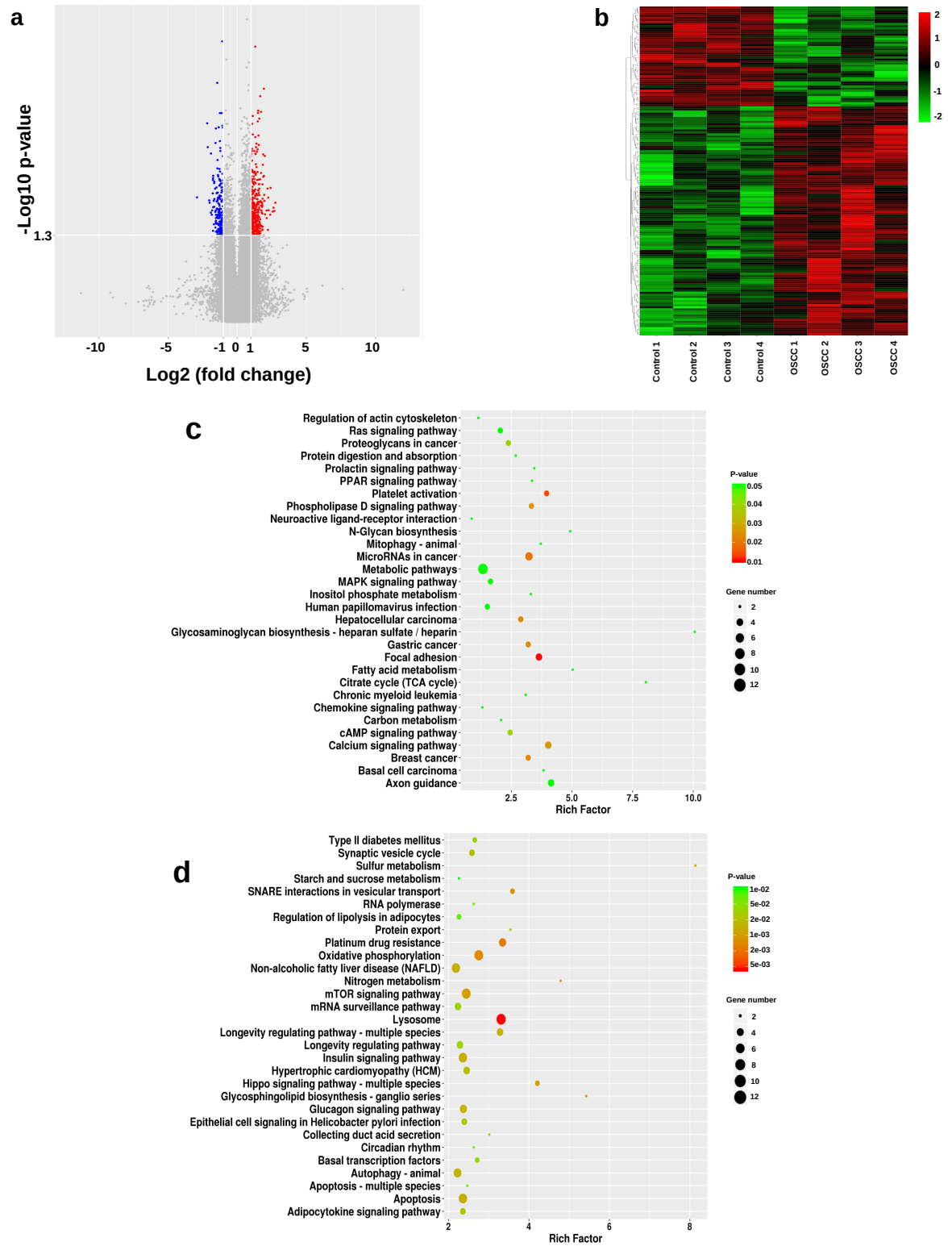

Fig. 1 Screening of differentially expressed lncRNAs and functional analysis of their target genes. (a) Volcano plot of all detected lncRNAs. Red, up-regulated lncRNAs in OSCC tissue vs. adjacent normal tissue. Blue, down-regulated lncRNAs in OSCC tissue vs. adjacent normal tissue. (b) Heat map of the differentially expressed lncRNAs. (c) The top 30 KEGG pathways of *cis*-target genes. (d) The top 30 KEGG pathways of *trans*-target genes.

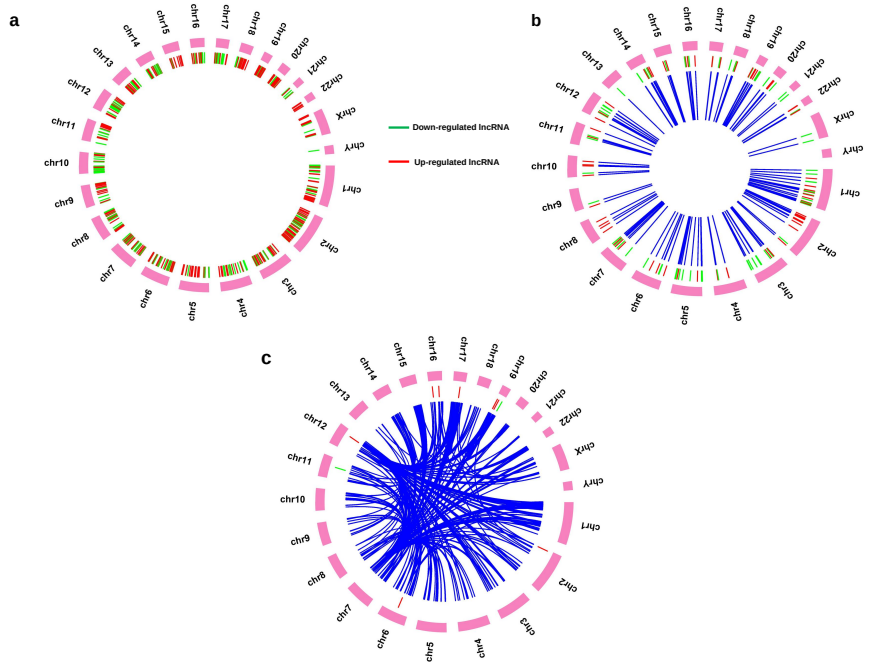

Fig. 2 Chromosomal distribution of differentially expressed lncRNAs. (a) Chromosome distribution of all differentially expressed lncRNAs ($n = 158$). (b) Chromosomal distribution of differentially expressed lncRNAs with *cis*-acting ($n = 85$). (c) Chromosomal distribution of differentially expressed lncRNAs with *trans*-acting ($n = 10$).

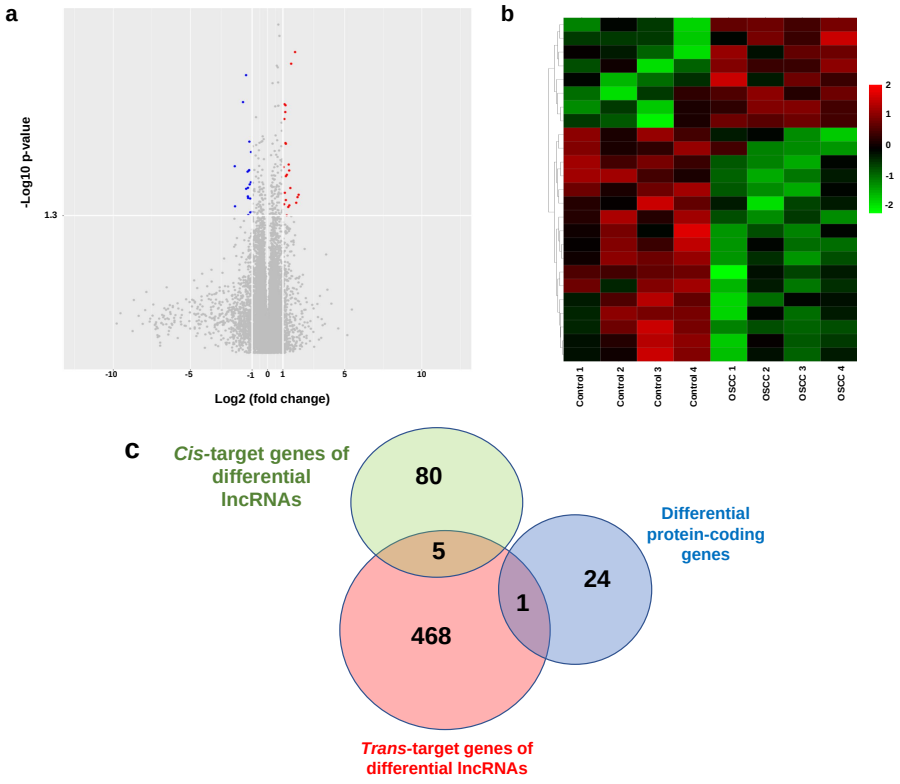

Fig. 3 Identification of *cis*- or *trans*-target differentially expressed protein-coding genes. (a) Volcano plot of all detected mRNAs. (b) Heat map of differentially expressed mRNAs. (c) Venn diagram for overlapping analysis of differentially expressed protein-coding genes and *cis*- or *trans*-target genes of differentially expressed lncRNAs.

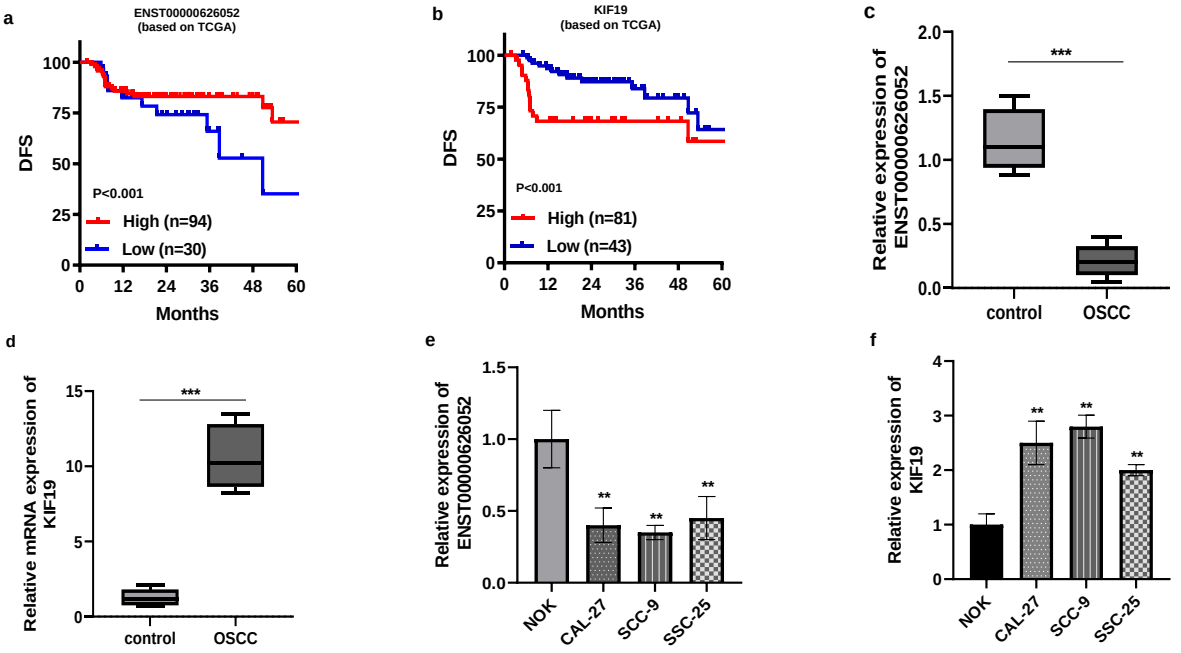

Fig. 4 Prognostic and expression analysis of ENSTa and KIF19. (a,b); Disease-free survival (DFS) analysis of ENSTa (a) and KIF19 (b) in OSCC patients based on TCGA database. (c,d); Relative expression of ENSTa (c) and KIF19 (d) in the 45 OSCC patients recruited in this study; *** $p < 0.001$. (e,f); Relative expression of ENSTa (e) and KIF19 (f) in normal human oral keratinocyte cell line (NOK) and OSCC cell lines (CAL-27, SCC-9 and SSC-25); ** $p < 0.01$, OSCC cells vs. NOK cell.

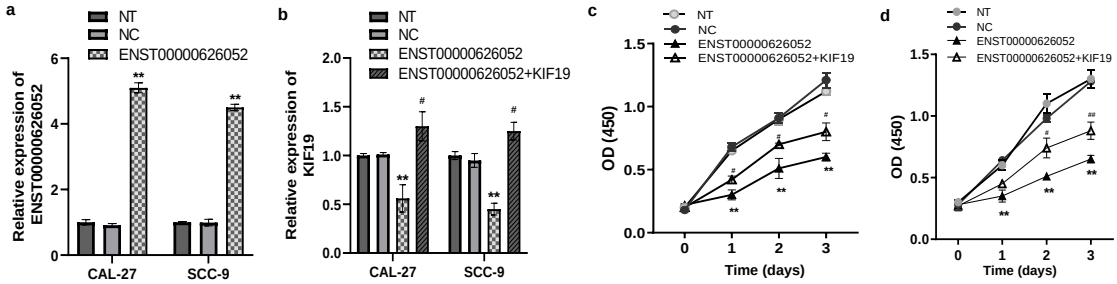

Fig. 5 Validation of *trans*-acting between ENSTa and KIF19, and the effect of ENSTa and KIF19 on cell proliferation. (a) Relative expression of ENSTa in CAL-27 and SCC-9 cells with/without ENSTa overexpression. (b) Relative expression of KIF19 in CAL-27 and SCC-9 cells. (c,d); Cell proliferation of CAL-27 (c) and SCC-9 (d) cells. NT, untransfection group; NC, pcDNA3.1 transfection group; ENSTa, pcDNA3.1- ENSTa transfection group; ENSTa+KIF19, pcDNA3.1-ENSTa and pcDNA3.1-KIF19 cotransfection group; ** $p < 0.01$, pcDNA3.1-ENSTa transfection group vs. pcDNA3.1 transfection group; $^{\#}$ $p < 0.05$, $^{\#\#}$ $p < 0.01$, pcDNA3.1-ENSTa and pcDNA3.1-KIF19 co-transfection group vs. pcDNA3.1-ENSTa transfection group.

ping analysis of *cis*- and *trans*-target genes of differentially expressed lncRNAs and differentially protein-coding genes. The results showed that KIF19 was a *trans*-acting gene of differentially expressed lncRNA (ENSTa), which was highly expressed in OSCC tissues and cells. KIF19 is a member of the kinesin superfamily proteins (KIFs) family. KIFs is a family of molecular motors with a total of 45 members, which can be divided into 14 subclasses [21]. Members of the KIFs family have highly conserved motor domains. KIFs family is not only involved in the transport of proteins and mRNA in cells, but also plays a key role in the spindle movement and the maintenance of chromosome stability during cell division [22–26]. KIFs family regulates the development of many cancers such as oral cancer, prostate cancer and liver cancer [26, 27]. KIF20B promotes tongue cancer progression by promoting the cell prolifera-

tion. Tongue cancer patients with high KIF20B expression have a poor clinicopathological outcome [26]. Up-regulation of KIF4A mRNA expression resulted in shorter overall survival time in prostate cancer [27]. KIF2C/4A/10/11/14/18B/20A/23 promote the proliferation of hepatocellular carcinoma cells, and high expression of these members leads to poor prognosis [28]. KIF19 is a member of the kinesin-8 subclass and is associated with ciliary vascular motility and vascular depolymerization [29]. Deficiency of KIF19 is associated with hydrocephalus, female infertility and autosomal dominant polycystic kidney disease [29, 30]. In recent years, KIF19 expression has been found to be associated with a cancer [31]. Li et al found that hepatocellular carcinoma patients with high expression of KIF19 had longer overall survival time [31]. To our best knowledge, the role of KIF19 in OSCC has not been reported. In this study, we found that KIF19 was highly expressed in OSCC tissues and cells. KIF19 was associated with a poor prognosis in OSCC patients. Furthermore, the down-regulation of KIF19 expression after ENSTa overexpression in OSCC cells was demonstrated by cellular level experiments, thus validating the *trans*-acting between ENSTa and KIF19. However, the more detailed regulatory mechanism between ENSTa and KIF19 still needs to be further explored.

In conclusion, a novel lncRNA, ENSTa, was identified, and its *trans*-acting differential protein encoding gene, KIF19, was screened out. ENSTa and its *trans*-target gene, KIF19, had a significant prognostic impact in OSCC. Subsequently, the *trans*-acting between ENSTa and KIF19 was verified by cellular assays. ENSTa inhibited OSCC cell proliferation, while KIF19 promoted OSCC cell proliferation. This study innovatively identified 2 potential biomarkers of OSCC, ENSTa and KIF19, and found a *trans*-acting between them, which is expected to provide new bio-targets for OSCC.

Appendix A. Supplementary data

Supplementary data associated with this article can be found at http://dx.doi.org/10.2306/scienceasia1513-1874.2022.047.

Acknowledgements: This work was supported by Hebei key project plan of medical science research (no. 20211538).

REFERENCES

1. Zhang B, Du W, Gan K, Fang Q, Zhang X (2019) Significance of the neutrophil-to-lymphocyte ratio in young patients with oral squamous cell carcinoma. *Cancer Manag Res* **11**, 7597–7603.
2. Li P, Fang Q, Yang Y, Chen D, Du W, Liu F, Luo R (2021) Survival significance of number of positive lymph nodes in oral squamous cell carcinoma stratified by p16. *Front Oncol* **11**, ID 545433.
3. Kawakami M, Yagi T, Takada K (2002) Maxillary expansion and protraction in correction of midface retrusion in a complete unilateral cleft lip and palate patient. *Angle Orthod* **72**, 355–361.
4. Chi AC, Day TA, Neville BW (2015) Oral cavity and oropharyngeal squamous cell carcinoma: an update. *CA Cancer J Clin* **65**, 401–421.
5. Xu L, Zhou H, Yi B, Hu H, Wu XY (2020) Plasma cell-free DNA for screening patients with benefit-assisted neoadjuvant chemotherapy for advanced gastric cancer. *ScienceAsia* **46**, 462–471.
6. Sun W, Zhang X, Ding X, Li H, Geng M, Xie Z, Wu H, Huang M (2015) Lactate dehydrogenase B is associated with the response to neoadjuvant chemotherapy in oral squamous cell carcinoma. *PLoS One* **10**, e0125976.
7. Brocklehurst PR, Baker SR, Speight PM (2010) Oral cancer screening: what have we learnt and what is there still to achieve? *Future Oncol* **6**, 299–304.
8. Ong YLR, Tivey D, Huang L, Sambrook P, Maddern G (2021) Factors affecting surgical mortality of oral squamous cell carcinoma resection. *Int J Oral Maxillofac Surg* **50**, 1–6.
9. Djebali S, Davis CA, Merkel A, Dobin A, Lassmann T, Mortazavi A, Tanzer A, Lagarde J, et al (2012) Landscape of transcription in human cells. *Nature* **489**, 101–108.
10. Huarte M (2015) The emerging role of lncRNAs in cancer. *Nat Med* **21**, 1253–1261.
11. Lee YS, Dutta A (2009) MicroRNAs in cancer. *Annu Rev Pathol* **4**, 199–227.
12. Patop IL, Kadener S (2018) circRNAs in Cancer. *Curr Opin Genet Dev* **48**, 121–127.
13. He X, Chai P, Li F, Zhang L, Zhou C, Yuan X, Li Y, Yang J, et al (2020) A novel lncRNA transcript, RBAT1, accelerates tumorigenesis through interacting with HNRNPL and *cis*-activating E2F3. *Mol Cancer* **19**, ID 115.
14. Cech TR, Steitz JA (2014) The noncoding RNA revolution-trashing old rules to forge new ones. *Cell* **157**, 77–94.
15. Kopp F, Mendell JT (2018) Functional classification and experimental dissection of long noncoding RNAs. *Cell* **172**, 393–407.
16. Diederichs S, Bartsch L, Berkmann JC, Frose K, Heitmann J, Hoppe C, Iggena D, Jazmati D, et al (2016) The dark matter of the cancer genome: aberrations in regulatory elements, untranslated regions, splice sites, non-coding RNA and synonymous mutations. *EMBO Mol Med* **8**, 442–457.
17. Stewart GL, Sage AP, Enfield KSS, Marshall EA, Cohn DE, Lam WL (2020) Deregulation of a *cis*-acting lncRNA in non-small cell lung cancer may control HMGA1 expression. *Front Genet* **11**, ID 615378.
18. Liu S, Zhang J, Yin L, Wang X, Zheng Y, Zhang Y, Gu J, Yang L, et al (2020) The lncRNA RUNX1-IT1 regulates C-FOS transcription by interacting with RUNX1 in the process of pancreatic cancer proliferation, migration and invasion. *Cell Death Dis* **11**, ID 412.
19. Chen C, Chen H, Zhang Y, Thomas HR, Frank MH, He Y, Xia R (2020) TBtools: an integrative toolkit developed for interactive analyses of big biological data. *Mol Plant* **13**, 1194–1202.
20. Pennacchiotti G, Valdes-Gutierrez F, Gonzalez-Arriagada WA, Montes HF, Parra JMR, Guida VA, Gomez SE, Guerrero-Gimenez ME, et al (2021) SPINK7 expression changes accompanied by HER2, P53 and RB1 can be relevant in predicting oral squamous cell carcinoma at a molecular level. *Sci Rep* **11**, ID 6939.

21. Diefenbach RJ, Mackay JP, Armati PJ, Cunningham AL (1998) The C-terminal region of the stalk domain of ubiquitous human kinesin heavy chain contains the binding site for kinesin light chain. *Biochemistry* **37**, 16663–16670.
22. Hirokawa N, Takemura R (2005) Molecular motors and mechanisms of directional transport in neurons. *Nat Rev Neurosci* **6**, 201–214.
23. Tipton AR, Wren JD, Daum JR, Siefert JC, Gorbsky GJ (2017) GTSE1 regulates spindle microtubule dynamics to control Aurora B kinase and Kif4A chromokinesin on chromosome arms. *J Cell Biol* **216**, 3117–3132.
24. Li QR, Yan XM, Guo L, Li J, Zang Y (2018) AMPK regulates anaphase central spindle length by phosphorylation of KIF4A. *J Mol Cell Biol* **10**, 2–17.
25. Hu CK, Coughlin M, Field CM, Mitchison TJ (2011) KIF4 regulates midzone length during cytokinesis. *Curr Biol* **21**, 815–824.
26. Li ZY, Wang ZX, Li CC (2019) Kinesin family member 20B regulates tongue cancer progression by promoting cell proliferation. *Mol Med Rep* **19**, 2202–2210.
27. Gao H, Chen X, Cai Q, Shang Z, Niu Y (2018) Increased KIF4A expression is a potential prognostic factor in prostate cancer. *Oncol Lett* **15**, 7941–7947.
28. Li X, Huang W, Huang W, Wei T, Zhu W, Chen G, Zhang J (2020) Kinesin family members KIF2C/4A/10/11/14/18B/20A/23 predict poor prognosis and promote cell proliferation in hepatocellular carcinoma. *Am J Transl Res* **12**, 1614–1639.
29. Wang D, Nitta R, Morikawa M, Yajima H, Inoue S, Shigematsu H, Kikkawa M, Hirokawa N (2016) Motility and microtubule depolymerization mechanisms of the Kinesin-8 motor, KIF19A. *Elife* **5**.
30. Skalicka K, Hrckova G, Vaska A, Baranyaiova A, Kovacs L (2018) Genetic defects in ciliary genes in autosomal dominant polycystic kidney disease. *World J Nephrol* **7**, 65–70.
31. Chen J, Li S, Zhou S, Cao S, Lou Y, Shen H, Yin J, Li G (2017) Kinesin superfamily protein expression and its association with progression and prognosis in hepatocellular carcinoma. *J Cancer Res Ther* **13**, 651–659.

Appendix A. Supplementary data

Table S1 Clinical characteristics of the 45 OSCC patients enrolled in this study.

Characteristic	Number of cases
Age	
< 60 years	25
$\geqslant 60$ years	20
Gender	
Male	21
Female	24
Tumor stage	
I–II	29
III–IV	16
Lymph node metastasis	
Yes	14
No	31